mathematics

MDPI

Article

Adaptive Secure Control for Leader-Follower Formation of Nonholonomic Mobile Robots in the Presence of Uncertainty and Deception Attacks

Bong-Seok Park [1] and Sung-Jin Yoo [2,*]

[1] Division of Electrical, Electronic, and Control Engineering, Institute of IT Convergence Technology, Kongju National University, Cheonan 31080, Korea; bspark@kongju.ac.kr
[2] School of Electrical and Electronics Engineering, Chung-Ang University, 84 Heukseok-Ro, Dongjak-Gu, Seoul 06974, Korea
* Correspondence: sjyoo@cau.ac.kr

Abstract: This paper addresses an adaptive secure control problem for the leader-follower formation of nonholonomic mobile robots in the presence of uncertainty and deception attacks. It is assumed that the false data of the leader robot's information attacked by the adversary is transmitted to the follower robot through the network, and the dynamic model of each robot has uncertainty, such as unknown nonlinearity and external disturbances. A robust, adaptive secure control strategy compensating for false data and uncertainty is developed to accomplish the desired formation of nonholonomic mobile robots. An adaptive compensation mechanism is derived to remove the effects of time-varying attack signals and system uncertainties in the proposed control scheme. Although unknown deception attacks are injected to the leader's velocities and the model nonlinearities of robots are unknown, the boundedness and convergence of formation tracking errors of the proposed adaptive control system are analyzed in the Lyapunov sense. The validity of the proposed scheme is verified via simulation results.

Keywords: secure control; corrupted leader signals; deception attack; leader-follower formation; nonholonomic mobile robot; neural network

Citation: Park, B.-S.; Yoo, S.-J. Adaptive Secure Control for Leader-Follower Formation of Nonholonomic Mobile Robots in the Presence of Uncertainty and Deception Attacks. *Mathematics* **2021**, *9*, 2190. https://doi.org/10.3390/math9182190

Academic Editor: António M. Lopes

Received: 23 July 2021
Accepted: 6 September 2021
Published: 7 September 2021

1. Introduction

Study efforts have actively proceeded to apply the cooperation technique of multi-robot systems to various areas, such as industries, commerce, and the military. For the operation of multi-robot systems, the robots are frequently connected through a network, which can be a target for attackers. Because exposure to a cyber-attack may result in critical loss of multi-robot systems, information security is essential and various methods, such as encryption techniques, intrusion detection systems, and secure control have been studied.

Cyber-attacks are largely divided into denial-of-service (DoS) disrupting services of a host connected to the network [1–3], a deception attack deceiving the data [4–6], and a replay attack delaying data transmission [7–9]. Among them, since a deception attack distorts the information of neighboring robots required to operate multi-robot systems, the robots that receive the wrong information cannot move according to the control objective, and finally, cause collaboration failure. Therefore, studies on secure control have been proposed. In [10], adaptive control architectures for linear dynamical systems with sensor uncertainty and attacks were presented. In [11,12], time-varying sensor and actuator attacks were estimated by the adaptive controllers. In [13], an adaptive event-triggered mechanism was proposed for the networked control systems (NCS) under deception attacks and stochastic nonlinearity. In [14], data quantization, DoS attacks, and deception attacks of the NCS were considered. In [15], the security correction control scheme based on an interconnected adaptive observer was proposed for stochastic cyber-physical systems subject to false data injection attacks. Because the above papers are

limited to linear systems, studies on nonlinear systems have been conducted. In [16], a neural-network-based controller was presented for uncertain nonlinear time-delay cyber-physical systems in the presence of sensor and actuator attacks. An approximation-based event-triggered control method was proposed to compensate for unknown injection data of lower-triangular nonlinear systems in [17]. In [18], an adaptive control scheme for second-order nonlinear systems was presented to deal with time-varying parameters and an unknown control direction brought by the injection and deception attacks. However, all these papers cannot be applied to nonholonomic mobile robots due to the underactuation problem. Although an adaptive resilient event-triggered control method at the kinematic level was proposed for single autonomous vehicles with DoS attacks [19], performance degradation due to uncertainty arising from the dynamic model is inevitable. Moreover, the deception attack problem was not considered in [19].

For the operation of multi-robot systems, formation control methods have been studied using the behavior-based approach [20], virtual structure [21], and leader-follower approach [22]. Although each approach has its advantages, the leader-follower approach has been widely used because of its simplicity, scalability, and reliability. Early studies on the leader-follower approach dealt with only the kinematics of mobile robots [22,23]. To consider model uncertainties and disturbances, studies were conducted that took into account the dynamics of mobile robots. The sliding mode control and adaptive neural network control problems were addressed to compensate for the uncertainty in [24,25], respectively. In recent years, formation control research has been conducted on connectivity preservation and collision avoidance between robots. In [26,27], formation control approaches using potential-like functions were presented. In [28], a dipolar navigation function was introduced to design the formation controller. In [29], a formation tracking method was proposed to avoid obstacles while maintaining connectivity. However, those studies mentioned above did not deal with the problem against deception attacks in the formation control design. For practical applications, it is significant to deal with the formation control of multiple mobile robots under deception attacks. This problem has not been addressed yet.

Accordingly, this paper proposes an adaptive secure control methodology for leader-follower formation of uncertain nonholonomic mobile robots in the presence of deception attacks of the leader's information. The leader's velocity information corrupted by unknown injected data is assumed to be transmitted to the follower robots through the network. A robust and resilient control design with adaptive attack compensation mechanisms is developed to compensate for time-varying velocity attacks where the radial basis function networks (RBFNs) are employed to deal with system uncertainties and external disturbances. Furthermore, in the proposed control design, the dynamic surface design technique is applied to circumvent the problem that the time derivatives of the virtual control laws are affected by unknown deception attack signals. It is proven that all closed-loop signals are uniformly ultimately bounded in the Lyapunov stability sense, and the formation errors are ensured for converging to an adjustable neighborhood of the origin. Finally, simulation results are given to verify the performance of the proposed theoretical approach.

Compared with the existing literature, the main contributions of this paper are as follows:

(i) To the best of the authors' knowledge, an adaptive secure control problem for leader-follower formation of nonholonomic mobile robots in the presence of deception attacks is the first trial of the formation control field of nonholonomic mobile robots. The secure formation control design and stability strategies using the adaptive technique are firstly established in this paper.

(ii) Compared with the related works in the literature, a robust, resilient control design with adaptive attack compensation mechanisms is firstly developed to compensate for time-varying velocity attacks of the leader. It is proven that all closed-loop signals

are uniformly ultimately bounded in the Lyapunov stability sense, and the formation errors are ensured for converging to an adjustable neighborhood of the origin.

The rest of this paper is organized as follows. In Section 2, the leader-follower model is introduced, and the adaptive secure control problem is formulated for achieving the desired formation of nonholonomic mobile robots with unknown deception velocity attacks. In Section 3, the proposed secure control strategy and its stability analysis are presented. In Section 4, simulation results are given. Finally, the conclusion of this paper is drawn in Section 5.

2. System Description and Problem Statement

2.1. Leader-Follower Model

In this paper, the leader-follower model, which is represented by the relative distance and angle between the leader i and follower j, is used for the formation of multiple mobile robots. If the leader-follower model is expressed using the relative distance and angle between the center positions of the leader and the follower, it is difficult to design the controller due to the lack of control inputs compared to the degrees of freedom. To address this problem, the leader-follower model shown in Figure 1 is used. This makes sense because the position of the sensor is different from the center position of the mobile robot in the practical application. From Figure 1, the relative distance l_{ij} and angle ϕ_{ij} between the leader i and the follower j measured by the sensor mounted on the follower j can be expressed as follows.

$$\begin{aligned} l_{ij} &= \sqrt{(x_i - x_j - d_j \cos\theta_j)^2 + (y_i - y_j - d_j \sin\theta_j)^2} \\ \phi_{ij} &= \theta_j - \arctan\left(\frac{y_i - y_j - d_j \sin\theta_j}{x_i - x_j - d_j \cos\theta_j}\right) \end{aligned} \tag{1}$$

where (x_n, y_n) and θ_n, $n = i, j$ denote the position and orientation of the robots, respectively, and d_j is the distance from the position of the follower j to the front sensor.

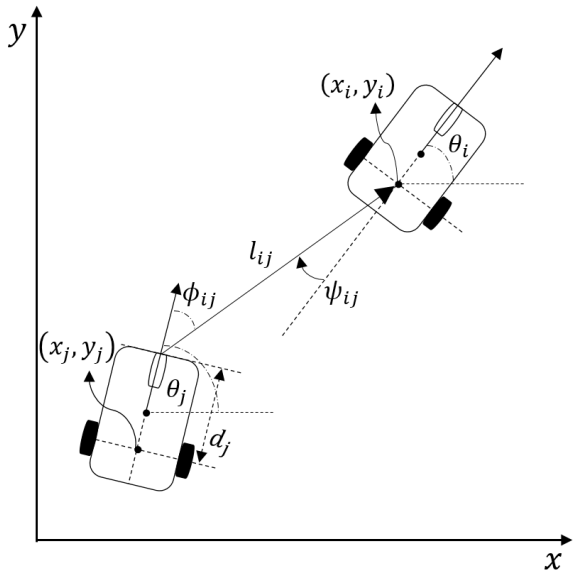

Figure 1. Leader-follower model.

The kinematics of the mobile robots are needed to derive the leader-follower model from (1), and the dynamics of the mobile robots are required to design the controller. The kinematics and dynamics of the mobile robots can be described by [30]

$$\dot{q}_n = \begin{bmatrix} \cos\theta_n & 0 \\ \sin\theta_n & 0 \\ 0 & 1 \end{bmatrix} \nu_n \tag{2}$$

$$\tau_n = M_n \dot{\nu}_n + C_n(\nu_n)\nu_n + D_n \nu_n + \tau_{d,n} \tag{3}$$

where $n = i, j$, $q_n = [x_n, y_n, \theta_n]^\top$; (x_n, y_n) is the position and θ_n is the heading angle, $\nu_n = [v_n, \omega_n]^\top$; v_n and ω_n are the linear and angular velocities, respectively, $\tau_{d,n}$ denotes the bounded external disturbance vector, and $\tau_n = [\tau_{1,n}, \tau_{2,n}]^\top$ is the control torque vector. In these expressions, the unknown matrices M_n, C_n, and D_n are defined as follows:

$$M_n = \begin{bmatrix} m_{1,n} & m_{2,n} \\ m_{1,n} & -m_{2,n} \end{bmatrix}, \; C_n(\nu_n) = \frac{r_n m_{b,n} c_n}{2R_n} \begin{bmatrix} 1 & -R_n \\ -1 & -R_n \end{bmatrix}, \; D_n = \frac{1}{r_n} \begin{bmatrix} d_{1,n} & R_n d_{1,n} \\ d_{2,n} & -R_n d_{2,n} \end{bmatrix},$$

where $m_{1,n} = r_n(m_{b,n} + 2m_{w,n})/2 + J_{w,n}/r_n$, $m_{2,n} = r_n J_n/(2R_n) + R_n J_{w,n}/r_n$, $J_n = m_{b,n}c_n^2 + 2m_{w,n}R_n^2 + J_{c,n} + J_{m,n}$, R_n and r_n denote the half of the width of the body and the radius of the wheel, respectively, c_n is the distance from the center of mass to the position of the nth mobile robot, $d_{1,n}$ and $d_{2,n}$ are the damping coefficients, $m_{b,n}$ and $m_{w,n}$ denote the mass of the body and the wheel, respectively, and $J_{c,n}$, $J_{w,n}$, and $J_{m,n}$ are the moments of inertia of the body, the wheel with a motor, and the wheel with the robot of a motor, respectively.

Substituting (2) into the time derivative of (1) yields the following leader-follower model [22]:

$$\begin{aligned} \dot{l}_{ij} &= v_i \cos\psi_{ij} - v_j \cos\phi_{ij} + d_j \omega_j \sin\phi_{ij} \\ \dot{\psi}_{ij} &= \omega_i - \frac{1}{l_{ij}} v_i \sin\psi_{ij} + \frac{1}{l_{ij}} v_j \sin\phi_{ij} + \frac{1}{l_{ij}} d_j \omega_j \cos\phi_{ij} \end{aligned} \tag{4}$$

where $\psi_{ij} = \phi_{ij} + \theta_i - \theta_j$.

2.2. Radial Basis Function Network

In this paper, we employ the radial basis function networks (RBFNs) to compensate the model uncertainty and external disturbance. The RBFN can approximate any continuous function $f(X)$ as follows: $f(X) = W^\top \Phi(X) + \varepsilon$ where X is the input vector, $W \in \mathbb{R}^{N_h}$ is the constant optimal weight vector, N_h is the node number, ε is the reconstruction error, and $\Phi(X) = [\varphi_1(X), \ldots, \varphi_{N_h}(X)]^\top$ is the Gaussian activation function defined by

$$\varphi_l(X) = \exp\left[\frac{-(X - \xi_l)^\top (X - \xi_l)}{\eta_l}\right], \; l = 1, \ldots, N_h$$

where ξ_l and η_l are the center and the width of the Gaussian function, respectively.

2.3. Problem Statement

To design the adaptive secure controller using the leader-follower model (4), the follower j requires the measurement data $(\theta_i, v_i, \omega_i)$ of the leader i. It can be corrupted by the adversary while it is transmitted over the communication network. Even though the transmitted data can be arbitrarily attacked by the adversary, the number of the corrupted data is limited due to the limited attack resources, such as [31]. In this paper, we assume that the leader velocities (v_i, ω_i) are corrupted by unknown attack signals. Thus, the follower j receives the corrupted data $(\bar{v}_i, \bar{\omega}_i)$ given by

$$\begin{aligned} \bar{v}_i &= v_i + a_{v,i} \\ \bar{\omega}_i &= \omega_i + a_{\omega,i} \end{aligned} \tag{5}$$

where $a_{v,i}$ and $a_{\omega,i}$ are the time-varying attack signals.

Therefore, the *control objective* of this paper is to design the torque input vector τ_j for the jth follower such that $\lim_{t\to\infty} |l_{ij} - l_{d,ij}| \leq \iota_j$ and $\lim_{t\to\infty} |\psi_{ij} - \psi_{d,ij}| \leq \iota_j$ are achieved in the environment with model uncertainty, external disturbance, and time-varying attack signals. Here, $l_{d,ij}$ and $\psi_{d,ij}$ denote the desired distance and angle, respectively, and ι_j is an arbitrarily small positive constant.

Assumption 1. *The following assumptions are used in this study.*

(i) *The leader's velocities (v_i, ω_i) and accelerations $(\dot{v}_i, \dot{\omega}_i)$ are bounded.*

(ii) *The external disturbance $\tau_{d,n}$ is bounded, such that $\|\tau_{d,n}\| \leq \bar{\tau}_{d,n}$, where $\bar{\tau}_{d,n}$ is an unknown positive constant.*

(iii) *The time-varying attack signals $a_{v,i}$ and $a_{\omega,i}$ are unknown and bounded, such that $|a_{v,i}| \leq \bar{a}_{v,i}$ and $|a_{\omega,i}| \leq \bar{a}_{\omega,i}$, where $\bar{a}_{v,i}$ and $\bar{a}_{\omega,i}$ are unknown positive constants.*

(iv) *The optimal weight vector W and reconstruction error ε are bounded, such that $\|W\| \leq \overline{W}$ and $|\varepsilon| \leq \bar{\varepsilon}$, where $\overline{W}$ and $\bar{\varepsilon}$ are unknown positive constants.*

(v) *The first derivatives of the desired distance $l_{d,ij}$ and angle $\psi_{d,ij}$ exist and are bounded.*

Remark 1. *The reasons for the validity of Assumption 1 are as follows.*

(i) *The follower j cannot follow the leader i unless the leader's velocity and acceleration are bounded. The unbounded leader's velocity and acceleration lead to the unstable operation of the leader i. Therefore, the leader's velocity and acceleration must be bounded for the leader-follower formation.*

(ii) *In a real environment, external disturbances, such as friction and wind, are bounded. If external disturbances are unbounded (i.e., infinite), the control problem cannot be formulated.*

(iii) *In real applications, since the defender can obtain some statistical information of the attack signal (e.g., extreme values) by monitoring the target online for some time, the bounded attack signals can ensure the concealment of the attacker [32]. Thus, Assumption 1-(iii) is reasonable in the secure control field.*

(iv) *Owing to the universal approximation property, the optimal weighting vector and reconstruction error are bounded (see [33,34]). Thus, Assumption 1-(iv) is reasonable in the control field using neural networks.*

(v) *$l_{d,ij}$ and $\psi_{d,ij}$ are the desired values chosen by the control designer for achieving the formation control objective. That is, they are the reference signals for the leader-follower control. Thus, they should be bounded. If they are infinite, the formation control problem cannot be formulated. In addition, for the continuous formation operation, $l_{d,ij}$ and $\psi_{d,ij}$ should be continuous and differentiable signals. Thus, Assumption 1-(v) is reasonable.*

The following Lemma will be used to prove the stability of the proposed control system.

Lemma 1 ([34])**.** *The following inequality is satisfied for any $\epsilon > 0$ and for any $\chi \in \mathbb{R}$*

$$0 \leq |\chi| - \chi \tanh\left(\frac{\chi}{\epsilon}\right) \leq \kappa\epsilon \tag{6}$$

where $\kappa = 0.2785$.

3. Controller Design

In this section, we design the controller to achieve the control objective under the assumption that the follower j receives the corrupted data $(\bar{v}_i, \bar{\omega}_i)$ from the leader i. The adaptive technique and neural networks are employed to deal with model uncertainty, external disturbance, and time-varying attack signals. The dynamic surface control (DSC) method [35] is used to design the controller at the dynamic level.

Let us define the errors as

$$e_{1,j} = l_{ij} - l_{d,ij} \tag{7}$$
$$e_{2,j} = \psi_{ij} - \psi_{d,ij} \tag{8}$$
$$e_{3,j} = \theta_{r,j} - \theta_j \tag{9}$$
$$e_{4,j} = \nu_j - \alpha_{f,j} \tag{10}$$
$$\varpi_j = [\varpi_{1,j}, \varpi_{2,j}]^\top = \alpha_{f,j} - \alpha_j \tag{11}$$

where $e_{4,j} = [e_{4,1,j}, e_{4,2,j}]^\top$, $\alpha_j = [\alpha_{1,j}, \alpha_{2,j}]^\top$ is the virtual control, $\alpha_{f,j} = [\alpha_{f,1,j}, \alpha_{f,2,j}]^\top$ is the filtered signal obtained by $\Gamma_j \dot{\alpha}_{f,j} + \alpha_{f,j} = \alpha_j$, $\alpha_{f,j}(0) = \alpha_j(0)$, Γ_j is a diagonal matrix and positive definite, and $\theta_{r,j}$ is the reference orientation to be defined later. In the leader-follower formation, the orientations of the leader i and the follower j cannot be equal while the formation is turning [25]. Thus, instead of following the orientation of the leader i, the reference orientation $\theta_{r,j}$ is required for the follower j.

Step 1: Substituting (2) and (4) into the time derivatives of (7)–(9) yields the following error dynamics,

$$\begin{aligned}
\dot{e}_{1,j} &= v_i \cos\psi_{ij} - v_j \cos\phi_{ij} + d_j \omega_j \sin\phi_{ij} - \dot{l}_{d,ij} \\
\dot{e}_{2,j} &= \omega_i - \frac{v_i}{l_{ij}} \sin\psi_{ij} + \frac{v_j}{l_{ij}} \sin\phi_{ij} + \frac{d_j}{l_{ij}} \omega_j \cos\phi_{ij} - \dot{\psi}_{d,ij} \\
\dot{e}_{3,j} &= \dot{\theta}_{r,j} - \omega_j.
\end{aligned} \tag{12}$$

Consider the Lyapunov function candidate as

$$V_{1,j} = \frac{1}{2}\left(e_{1,j}^2 + e_{2,j}^2 + e_{3,j}^2 + \frac{1}{\gamma_{v,j}} \tilde{a}_{v,j}^2 + \frac{1}{\gamma_{\omega,j}} \tilde{a}_{\omega,j}^2\right) \tag{13}$$

where $\gamma_{v,j}$ and $\gamma_{\omega,j}$ are positive constants, $\tilde{a}_{v,j} = \bar{a}_{v,i} - \hat{a}_{v,j}$, $\tilde{a}_{\omega,j} = \bar{a}_{\omega,i} - \hat{a}_{\omega,j}$, and $\hat{a}_{v,j}$ and $\hat{a}_{\omega,j}$ are the estimates of $\bar{a}_{v,i}$ and $\bar{a}_{\omega,i}$, respectively. By Assumption 1-(iii) and the inequality, we obtain the time derivative of (13) along (10)–(12) as follows:

$$\begin{aligned}
\dot{V}_{1,j} =& e_{1,j}\Big(\bar{v}_i \cos\psi_{ij} - a_{v,i} \cos\psi_{ij} - \dot{l}_{d,ij} - (e_{4,1,j} + \alpha_{1,j} + \varpi_{1,j}) \cos\phi_{ij} \\
&+ d_j (e_{4,2,j} + \alpha_{2,j} + \varpi_{2,j}) \sin\phi_{ij}\Big) \\
&+ e_{2,j}\Big(\bar{\omega}_i - \frac{\bar{v}_i}{l_{ij}} \sin\psi_{ij} - a_{\omega,i} + \frac{a_{v,i}}{l_{ij}} \sin\psi_{ij} - \dot{\psi}_{d,ij} + \frac{e_{4,1,j} + \alpha_{1,j} + \varpi_{1,j}}{l_{ij}} \sin\phi_{ij} \\
&+ \frac{d_j}{l_{ij}} (e_{4,2,j} + \alpha_{2,j} + \varpi_{2,j}) \cos\phi_{ij}\Big) \\
&+ e_{3,j}(\dot{\theta}_{r,j} - e_{4,2,j} - \alpha_{2,j} - \varpi_{2,j}) - \frac{1}{\gamma_{v,j}} \tilde{a}_{v,j} \dot{\hat{a}}_{v,j} - \frac{1}{\gamma_{\omega,j}} \tilde{a}_{\omega,j} \dot{\hat{a}}_{\omega,j} \\
\leq& e_{1,j}\Big(\bar{v}_i \cos\psi_{ij} - \dot{l}_{d,ij} - (e_{4,1,j} + \alpha_{1,j} + \varpi_{1,j}) \cos\phi_{ij} + d_j (e_{4,2,j} + \alpha_{2,j} + \varpi_{2,j}) \sin\phi_{ij}\Big) \\
&+ e_{2,j}\Big(\bar{\omega}_i - \frac{\bar{v}_i}{l_{ij}} \sin\psi_{ij} + \frac{e_{4,1,j} + \alpha_{1,j} + \varpi_{1,j}}{l_{ij}} \sin\phi_{ij}
\end{aligned}$$

$$+\frac{d_j}{l_{ij}}(e_{4,2,j}+\alpha_{2,j}+\varpi_{2,j})\cos\phi_{ij}-\dot{\psi}_{d,ij}\Big)$$
$$+|\hat{a}_{v,j}e_{1,j}|+\tilde{a}_{v,j}|e_{1,j}|+|\hat{a}_{\omega,j}e_{2,j}|+\tilde{a}_{\omega,j}|e_{2,j}|+\frac{|\hat{a}_{v,j}e_{2,j}|+\tilde{a}_{v,j}|e_{2,j}|}{l_{ij}}$$
$$+e_{3,j}(\dot{\theta}_{r,j}-e_{4,2,j}-\alpha_{2,j}-\varpi_{2,j})-\frac{1}{\gamma_{v,j}}\tilde{a}_{v,j}\dot{\hat{a}}_{v,j}-\frac{1}{\gamma_{\omega,j}}\tilde{a}_{\omega,j}\dot{\hat{a}}_{\omega,j}. \tag{14}$$

The virtual controls $\alpha_{1,j}$ and $\alpha_{2,j}$ are chosen as

$$\alpha_{1,j}=\zeta_{1,j}\cos\phi_{ij}-l_{ij}\zeta_{2,j}\sin\phi_{ij}$$
$$\alpha_{2,j}=-\frac{\zeta_{1,j}}{d_j}\sin\phi_{ij}-\frac{l_{ij}}{d_j}\zeta_{2,j}\cos\phi_{ij} \tag{15}$$

and the reference orientation is updated by

$$\dot{\theta}_{r,j}=\alpha_{2,j}-k_{3,j}e_{3,j} \tag{16}$$

where

$$\zeta_{1,j}=k_{1,j}e_{1,j}+\hat{a}_{v,j}\tanh\left(\frac{\hat{a}_{v,j}e_{1,j}}{\epsilon_j}\right)-\dot{l}_{d,ij}+\bar{v}_i\cos\psi_{ij}$$
$$\zeta_{2,j}=k_{2,j}e_{2,j}+\bar{\omega}_i-\frac{\bar{v}_i}{l_{ij}}\sin\psi_{ij}-\dot{\psi}_{d,ij}+\frac{\hat{a}_{v,j}}{l_{ij}}\tanh\left(\frac{\hat{a}_{v,j}e_{2,j}}{\epsilon_j l_{ij}}\right)+\hat{a}_{\omega,j}\tanh\left(\frac{\hat{a}_{\omega,j}e_{2,j}}{\epsilon_j}\right)$$

with positive constants $k_{1,j}$, $k_{2,j}$, $k_{3,j}$, and ϵ_j. Substituting (15) and (16) into (14) and using Lemma 1 yield

$$\dot{V}_{1,j}\leq -k_{1,j}e_{1,j}^2-k_{2,j}e_{2,j}^2-k_{3,j}e_{3,j}^2+3\kappa\epsilon_j-e_{1,j}(e_{4,1,j}\cos\phi_{ij}-d_je_{4,2,j}\sin\phi_{ij})$$
$$+\frac{e_{2,j}}{l_{ij}}(e_{4,1,j}\sin\phi_{ij}+d_je_{4,2,j}\cos\phi_{ij})-e_{3,j}e_{4,2,j}-e_{1,j}(\varpi_{1,j}\cos\phi_{ij}-d_j\varpi_{2,j}\sin\phi_{ij})$$
$$+\frac{e_{2,j}}{l_{ij}}(\varpi_{1,j}\sin\phi_{ij}+d_j\varpi_{2,j}\cos\phi_{ij})-e_{3,j}\varpi_{2,j}+\tilde{a}_{v,j}\left(|e_{1,j}|+\frac{|e_{2,j}|}{l_{ij}}-\frac{1}{\gamma_{v,j}}\dot{\hat{a}}_{v,j}\right)$$
$$+\tilde{a}_{\omega,j}\left(|e_{2,j}|-\frac{1}{\gamma_{\omega,j}}\dot{\hat{a}}_{\omega,j}\right) \tag{17}$$

where from Lemma 1, the following inequalities are used:

$$|\hat{a}_{v,j}e_{1,j}|-\hat{a}_{v,j}e_{1,j}\tanh\left(\frac{\hat{a}_{v,j}e_{1,j}}{\epsilon_j}\right)\leq\kappa\epsilon_j$$
$$|\hat{a}_{\omega,j}e_{2,j}|-\hat{a}_{\omega,j}e_{2,j}\tanh\left(\frac{\hat{a}_{\omega,j}e_{2,j}}{\epsilon_j}\right)\leq\kappa\epsilon_j$$
$$\frac{|\hat{a}_{v,j}e_{2,j}|}{l_{ij}}-\frac{\hat{a}_{v,j}e_{2,j}}{l_{ij}}\tanh\left(\frac{\hat{a}_{v,j}e_{2,j}}{\epsilon_j l_{ij}}\right)\leq\kappa\epsilon_j.$$

We choose the adaptation laws as

$$\dot{\hat{a}}_{v,j}=\gamma_{v,j}\left(|e_{1,j}|+\frac{|e_{2,j}|}{l_{ij}}\right)-\gamma_{v,j}\sigma_{1,j}\hat{a}_{v,j}$$
$$\dot{\hat{a}}_{\omega,j}=\gamma_{\omega,j}|e_{2,j}|-\gamma_{\omega,j}\sigma_{2,j}\hat{a}_{\omega,j} \tag{18}$$

where $\sigma_{1,j}$ and $\sigma_{2,j}$ are positive constants.

Step 2: The time derivative of (10) along (3) is

$$\dot{e}_{4,j} = M_j^{-1}(-C_j(\nu_j)\nu_j - D_j\nu_j - \tau_{d,j} + \tau_j) - \dot{\alpha}_{f,j}. \tag{19}$$

Multiplying B_jM_j both sides of (19) yields

$$\overline{M}_j\dot{e}_{4,j} = -B_j(C_j(\nu_j)\nu_j + D_j\nu_j + M_j\dot{\alpha}_{f,j}) - B_j\tau_{d,j} + B_j\tau_j \tag{20}$$

where

$$\overline{M}_j = B_jM_j,\ B_j = \frac{1}{2}\begin{bmatrix}1 & 1\\ 1 & -1\end{bmatrix}.$$

Note that there exists the inverse of B_j, and the constant matrix $\overline{M}_j$ is positive definite.

Consider the Lyapunov function candidate as

$$V_{2,j} = \frac{1}{2}\left(e_{4,j}^\top\overline{M}_je_{4,j} + \sum_{l=1}^{2}\frac{1}{\gamma_{l,j}}\widetilde{W}_{l,j}^\top\widetilde{W}_{l,j} + \varpi_j^\top\varpi_j\right) \tag{21}$$

where $\gamma_{l,j} > 0$, $\widetilde{W}_{l,j} = W_{l,j} - \widehat{W}_{l,j}$, $W_{l,j}$ is the constant optimal weight vector, and $\widehat{W}_{l,j}$ is the estimate of $W_{l,j}$. By Assumption 1(ii), the time derivative of (21) along (20) yields

$$\begin{aligned}\dot{V}_{2,j} =& e_{4,j}^\top(-B_j(C_j(\nu_j)\nu_j + D_j\nu_j + M_j\dot{\alpha}_{f,j}) - B_j\tau_{d,j} + B_j\tau_j)\\ &- \sum_{l=1}^{2}\frac{1}{\gamma_{l,j}}\widetilde{W}_{l,j}^\top\dot{\widehat{W}}_{l,j} - \varpi_j^\top\Gamma_j^{-1}\varpi_j - \varpi_j^\top\dot{\alpha}_j\\ \leq& e_{4,j}^\top(f_j(X_j) + B_j\tau_j) - \sum_{l=1}^{2}\frac{1}{\gamma_{l,j}}\widetilde{W}_{l,j}^\top\dot{\widehat{W}}_{l,j} - \varpi_j^\top\Gamma_j^{-1}\varpi_j - \varpi_j^\top\dot{\alpha}_j + \frac{\varsigma_j}{2}\end{aligned} \tag{22}$$

where $f_j(X_j) = [f_{1,j}, f_{2,j}]^\top = -B_j(C_j(\nu_j)\nu_j + D_j\nu_j - M_j\Gamma^{-1}\varpi_j) + \bar{\tau}_{d,j}^2e_{4,j}/(2\varsigma_j)$ with $X_j = [\nu_j^\top, \varpi_j^\top, e_{4,j}^\top]^\top$ and a constant $\varsigma_j > 0$. Note that the continuous functions $f_{n,j}$ for $n = 1, 2$ can be approximated by RBFNs as follows: $f_{n,j}(X_j) = W_{n,j}^\top\Phi_j + \varepsilon_{n,j}$.

Remark 2. *The backstepping technique cannot be applied to the secure control problem concerned in this paper because the time derivative of the virtual control α_j includes the unknown time-varying attack signals. Thus, the term $\dot{\alpha}_j$ cannot be removed by the actual control torque τ_j of the follower j. To overcome this problem, we employ the dynamic surface control method that can replace the time derivative of α_j with the first-order filtered signal term $\Gamma_j^{-1}\varpi_j$ in the neural network approximator.*

We chose the actual control inputs and update laws as

$$\tau_j = -B_j^{-1}(\widehat{W}_j^\top\Phi_j(X_j) + k_{4,j}e_{4,j} + \Lambda_j) \tag{23}$$

$$\begin{aligned}\dot{\widehat{W}}_{1,j} &= \gamma_{1,j}\Phi_je_{4,1,j} - \gamma_{1,j}\sigma_{3,j}\widehat{W}_{1,j}\\ \dot{\widehat{W}}_{2,j} &= \gamma_{2,j}\Phi_je_{4,2,j} - \gamma_{2,j}\sigma_{4,j}\widehat{W}_{2,j}\end{aligned} \tag{24}$$

where $k_{4,j}$, $\sigma_{3,4}$, and $\sigma_{4,j}$ are positive constants, and

$$\widehat{W}_j = [\widehat{W}_{1,j}, \widehat{W}_{2,j}],$$
$$\Lambda_j = \begin{bmatrix}-e_{1,j}\cos\phi_{ij} + \frac{e_{2,j}}{l_{ij}}\sin\phi_{ij}\\ d_je_{1,j}\sin\phi_{ij} + \frac{d_j}{l_{ij}}e_{2,j}\cos\phi_{ij} - e_{3,j}\end{bmatrix}.$$

Consider the Lyapunov function candidate $V_{T,j} = V_{1,j} + V_{2,j}$. Then, the following theorem gives the main result of this paper.

Theorem 1. *Assume that the transmitted leader signals (v_i, ω_i) are attacked by the adversary, and consider the leader-follower model (4) controlled by the proposed controller (23) with the update laws (18) and (24) under Assumption 1. For any initial conditions such that $V_{T,j}(0) \leq \beta_{0,j}$ where $\beta_{0,j}$ is a positive constant, there exist $k_{1,j}$, $k_{2,j}$, $k_{3,j}$, $\gamma_{v,j}$, $\gamma_{\omega,j}$, $\gamma_{1,j}$, $\gamma_{2,j}$, and Γ_j such that $V_{T,j}(t) \leq \beta_{0,j}$, $\forall t \geq 0$. Furthermore, the control objective is achieved, namely, $\lim_{t\to\infty} |l_{ij} - l_{d,ij}| \leq \iota_j$ and $\lim_{t\to\infty} |\psi_{ij} - \psi_{d,ij}| \leq \iota_j$.*

Proof. Substituting (18), (23), and (24) into the time derivative of $V_{T,j}$ along (17) and (22), we have

$$\begin{aligned}\dot{V}_{T,j} =& -k_{1,j}e_{1,j}^2 - k_{2,j}e_{2,j}^2 - k_{3,j}e_{3,j}^2 - k_{4,j}e_{4,j}^\top e_{4,j} + \left(|e_{1,j}| + \frac{1}{l_{ij}}|e_{2,j}|\right)(|\omega_{1,j}| + d_j|\omega_{2,j}|) \\ &+ |e_{3,j}||\omega_{2,j}| + \sigma_{1,j}\tilde{a}_{v,j}\hat{a}_{v,j} + \sigma_{2,j}\tilde{a}_{\omega,j}\hat{a}_{\omega,j} + e_{4,j}^\top\varepsilon_j - \omega_j^\top\Gamma_j^{-1}\omega_j + \|\omega_j\|\|\dot{\alpha}_j\| \\ &+ \sigma_{3,j}\widetilde{W}_{1,j}^\top\widehat{W}_{1,j} + \sigma_{4,j}\widetilde{W}_{2,j}^\top\widehat{W}_{2,j} + 3\kappa\epsilon_j + \frac{\varsigma_j}{2} \end{aligned} \tag{25}$$

where $\varepsilon_j = [\varepsilon_{1,j}, \varepsilon_{2,j}]^\top$. From the definition of α_j and Assumption 1(i), it follows that

$$\|\dot{\alpha}_j\| \leq h_j(e_{1,j}, e_{2,j}, e_{4,j}, \omega_j, \tilde{a}_{v,j}, \tilde{a}_{\omega,j}) \tag{26}$$

for some continuous function h_j. Consider the set $\Omega_j := \{e_{1,j}^2 + e_{2,j}^2 + e_{4,j}^\top\overline{M}_j e_{4,j} + \tilde{a}_{v,j}^2/\gamma_{v,j} + \tilde{a}_{\omega,j}^2/\gamma_{\omega,j} + \omega_j^\top\omega_j \leq 2\beta_{0,j}\}$. There exists a positive constant $\bar{\beta}_j$ such that $\|\dot{\alpha}_j\| \leq \bar{\beta}_j$ on Ω_j. By Assumption 1(iv) and Young's inequality, (25) can be written as

$$\begin{aligned}\dot{V}_{T,j} \leq& -(k_{1,j}-1)e_{1,j}^2 - (k_{2,j}-1)e_{2,j}^2 - (k_{3,j}-1)e_{3,j}^2 - (k_{4,j}-1)e_{4,j}^\top e_{4,j} - \frac{\sigma_{1,j}}{2}\tilde{a}_{v,j}^2 - \frac{\sigma_{2,j}}{2}\tilde{a}_{\omega,j}^2 \\ &- \omega_j^\top\left(\Gamma_j^{-1} - \frac{\bar{\beta}_j^2}{2\delta_j}I - \Upsilon_j\right)\omega_j - \frac{\sigma_{3,j}}{2}\widetilde{W}_{1,j}^\top\widetilde{W}_{1,j} - \frac{\sigma_{4,j}}{2}\widetilde{W}_{2,j}^\top\widetilde{W}_{2,j} - \frac{\|\omega_j\|^2\bar{\beta}_j^2}{2\delta_j}\left(1 - \frac{h_j^2}{\bar{\beta}_j^2}\right) \\ &+ \frac{\delta_j}{2} + 3\kappa\epsilon_j + \frac{\sigma_{1,j}}{2}\bar{a}_{v,i}^2 + \frac{\sigma_{2,j}}{2}\bar{a}_{\omega,i}^2 + \frac{\sigma_{3,j}}{2}\overline{W}_{1,j}^2 + \frac{\sigma_{4,j}}{2}\overline{W}_{2,j}^2 + \frac{\bar{\varepsilon}_{1,j}^2}{4} + \frac{\bar{\varepsilon}_{2,j}^2}{4} + \frac{\varsigma_j}{2} \end{aligned} \tag{27}$$

where I is a 2×2 identity matrix, δ_j is a positive constant, and

$$\Upsilon_j = \begin{bmatrix} \frac{1}{2} + \frac{1}{2l_{ij}^2} & 0 \\ 0 & \frac{d_j^2}{2} + \frac{d_j^2}{2l_{ij}^2} + \frac{1}{4} \end{bmatrix}.$$

If we choose $k_{l,j} = 1 + k_{l,j}^*$ and $\Gamma_j^{-1} = \bar{\beta}_j^2 I/(2\delta_j) + \Upsilon_j + \Gamma_j^*$ where $k_{l,j}^* > 0$, $\Gamma_j^* > 0$, and $l = 1, \ldots, 4$, then (27) is expressed as

$$\dot{V}_{T,j} \leq -2\mu_{0,j}V_{T,j} + \mu_{1,j} - \frac{\|\omega_j\|^2\bar{\beta}_j^2}{2\delta_j}\left(1 - \frac{h_j^2}{\bar{\beta}_j^2}\right) \tag{28}$$

where $\mu_{0,j} = \min\{k_{1,j}^*, k_{2,j}^*, k_{3,j}^*, \lambda_{\min}(\overline{M}_j^{-1})k_{4,j}^*, \gamma_{v,j}\sigma_{1,j}/2, \gamma_{\omega,j}\sigma_{2,j}/2, \lambda_{\min}(\Gamma_j^*), \gamma_{1,j}\sigma_{3,j}/2, \gamma_{2,j}\sigma_{4,j}/2\}$, $\mu_{1,j} = \delta_j/2 + 3\kappa\epsilon_j + \sigma_{1,j}\bar{a}_{v,i}^2/2 + \sigma_{2,j}\bar{a}_{\omega,i}^2/2 + \sigma_{3,j}\overline{W}_{1,j}^2/2 + \sigma_{4,j}\overline{W}_{2,j}^2/2 + \bar{\varepsilon}_{1,j}^2/4 + \bar{\varepsilon}_{2,j}^2/4 + \varsigma_j/2$, and $\lambda_{\min}(\cdot)$ is a minimum eigenvalue of $(\cdot)$. On $V_{T,j} = \beta_{0,j}$, $h_j \leq \bar{\beta}_j$. Therefore, $\dot{V}_{T,j} \leq -2\mu_{0,j}V_{T,j} + \mu_{1,j}$. If $\mu_{0,j} > \mu_{1,j}/(2\beta_{0,j})$, then $\dot{V}_{T,j} \leq 0$ on $V_{T,j} = \beta_{0,j}$. This implies that there exist $k_{1,j}$, $k_{2,j}$, $k_{3,j}$, $\gamma_{v,j}$, $\gamma_{\omega,j}$, $\gamma_{1,j}$, $\gamma_{2,j}$, and Γ_j such that $V_{T,j} \leq \beta_{0,j}$, $\forall t \geq 0$. Furthermore, fixing $\sigma_{l,j}$ for $l = 1, \ldots, 4$ and increasing $\mu_{0,j}$ allow $V_{T,j}$ to be within the arbitrarily small bound $\mu_{1,j}/(2\mu_{0,j})$. Therefore, the control objective is achieved, that is, $\lim_{t\to\infty} |l_{ij} - l_{d,ij}| \leq \iota_j$ and $\lim_{t\to\infty} |\psi_{ij} - \psi_{d,ij}| \leq \iota_j$, where $\iota_j = \sqrt{\mu_{1,j}/\mu_{0,j}}$. This completes the proof. □

Remark 3. *Theorem 1 proves the stability of the jth robot. For the formation of N mobile robots, a stability analysis for all robots, called formation stability [25], should be given. Because the formation stability can be analyzed using the sum of the Lyapunov candidate $V_{T,j}$ for all j, it can be easily proven using the proof of Theorem 1. However, the sum of errors can be large, as many layers exist. A leader-to-formation stability (LFS) [36], which provides performance measures that can be calculated analytically, can be applied to analyze a stability property of leader-following formations. Using the LFS allows the calculation of worst-case ultimate error bounds. Thus, this can be used to check a particular formation design. For example, if the LFS measure is unacceptable, the stability of the formation can be improved by adjusting the reference trajectory or formation architecture.*

4. Simulation Results

In this section, we simulate five robots to demonstrate the performance of the proposed control scheme. Figure 2 shows the desired formation and information flow. The model parameters of each robot follow closely [30]. The initial postures of all robots are set to $q_0 = [0, 0, \pi/4]^\top$, $q_1 = [-3, -3, \pi/2]^\top$, $q_2 = [3, -3, \pi/2]^\top$, $q_3 = [-6, -3, \pi/2]^\top$, and $q_4 = [6, -3, \pi/2]^\top$. The external disturbances are given by $\tau_{d,j} = [0.7\cos(1.5t), 1.2\sin(0.5t)]^\top$. The time-varying attack signals are set to $a_{v,n} = \sin(\pi t/5)$ and $a_{\omega,n} = \cos(\pi t/5)$, where $n = 0, 1, 2$. The design parameters are chosen as $\gamma_{v,j} = \gamma_{\omega,j} = \gamma_{1,j} = \gamma_{2,j} = 5$, $k_{n,j} = 5$, $\sigma_{n,j} = 0.002$, $\Gamma_j = \mathrm{diag}[0.01, 0.01]$, and $\epsilon_j = 0.5$ where $n = 1, \ldots, 4$. We assume that the robot 0 moves autonomously and the trajectory is generated by (2). The velocities of the robot 0 are chosen as follows: $\nu_0 = [0.25(1 - \cos(\pi t/5)), 0]^\top$ for $0 \le t < 5$, $\nu_0 = [0.5, 0]^\top$ for $5 \le t < 25$, $\nu_0 = [0.5, 0.2\cos(2\pi t/20)]^\top$ for $25 \le t < 45$, and $\nu_0 = [0.5, 0]^\top$ for $t \ge 45$.

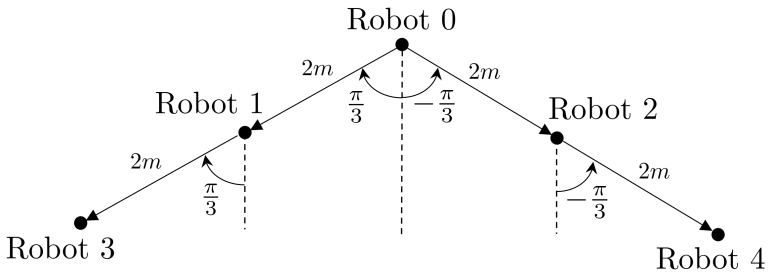

Figure 2. Desired formation and information flow.

Figures 3–5 show the simulation results. As shown in Figures 3 and 4, the desired formation is achieved for straight and curved paths, and the formation errors converge to nearly zero. As shown in Figure 4, both the distance and angle errors that occur at the starting point drop quickly in less than a few seconds. Thus, there are design parameters that can achieve the desired formation, as mentioned in Theorem 1. This implies that the theoretical results of Theorem 1 are valid. Therefore, it can be seen from Theorem 1 that increasing the design parameters can reduce the bounds of the error and speed up the convergence rate. Figure 5 depicts the control torques of all robots. Figures 6 and 7 show the estimates of the attack signals and the outputs of the RBFNs. From Figures 6 and 7, we can see that the bounds of the attack signals and unknown nonlinearities of the follower dynamics are compensated by the proposed adaptive laws and the adaptive neural network approximators, respectively. To consider various attack signals, the simulation with impulse attack signals is conducted. In this case, the impulse attack signals are chosen as: $a_{v,n} = 0.5$ and $a_{\omega,n} = 0$ at $t = 20$ s, $a_{v,n} = 1$ and $a_{\omega,n} = 0.5$ at $t = 40$ s, and $a_{v,n} = -1$ and $a_{\omega,n} = -0.5$ at $t = 60$ s, where $n = 0, 1, 2$. Figure 8 shows the simulation results. It can be seen that the formation tracking errors converge to nearly zero even though the control torques are affected by impulse attack signals. From the simulation results, it can be concluded that the proposed scheme is effective in achieving the desired formation of uncertain mobile robots in the presence of unknown attack signals.

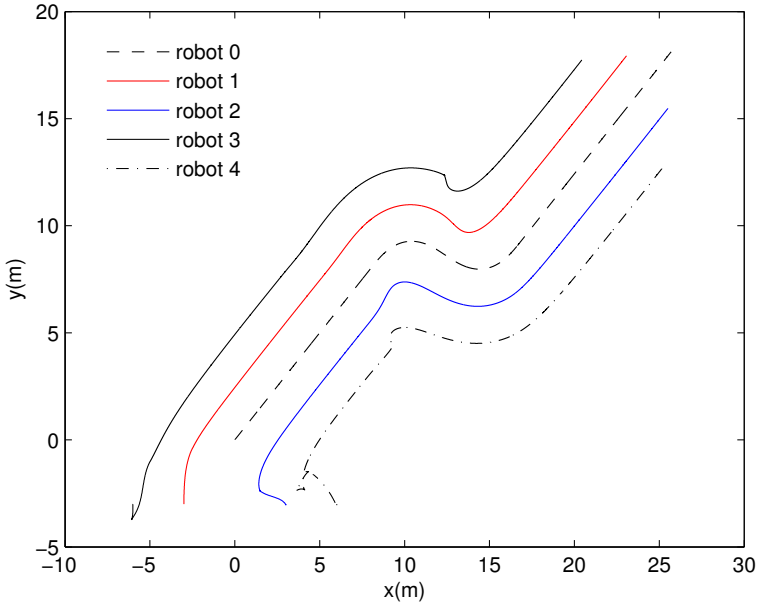

Figure 3. Formation tracking result.

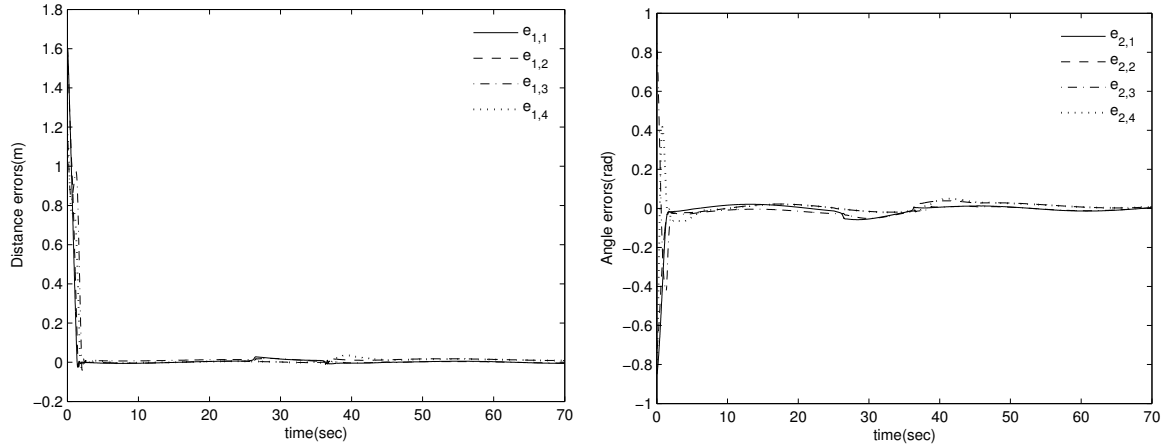

(**a**) Distance errors $e_{1,j}$ (**b**) Angle errors $e_{2,j}$

Figure 4. Formation errors.

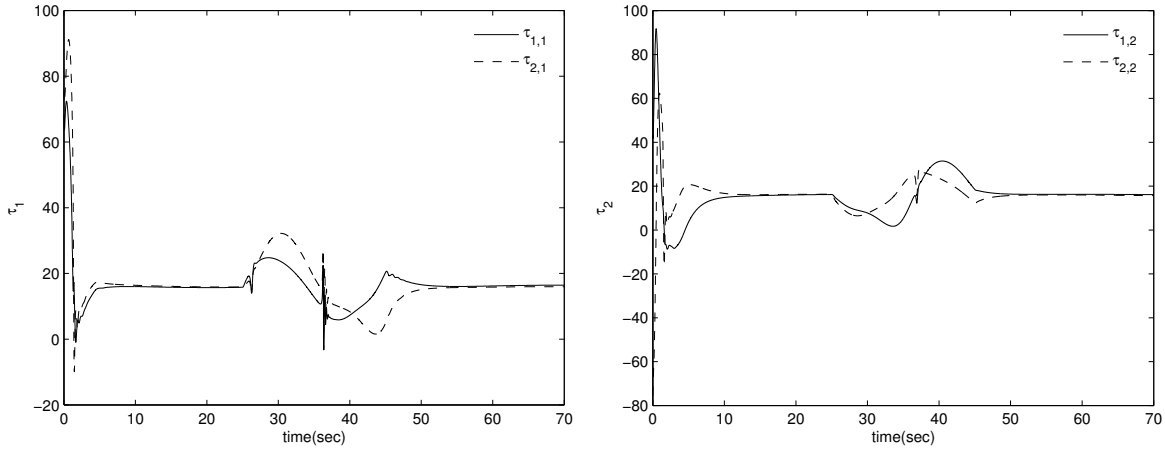

(**a**) τ_1 (**b**) τ_2

Figure 5. *Cont.*

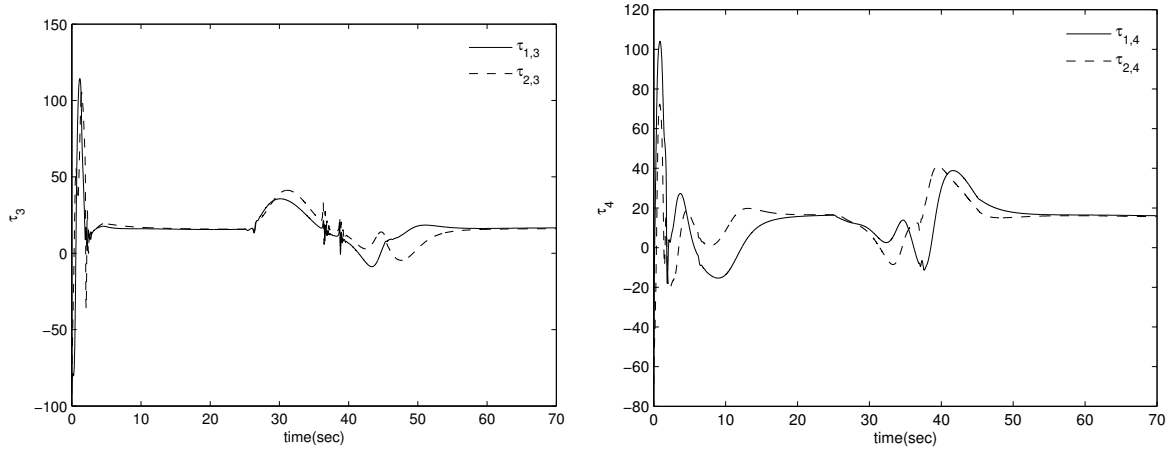

(**c**) τ_3 (**d**) τ_4

Figure 5. Control torque τ_j.

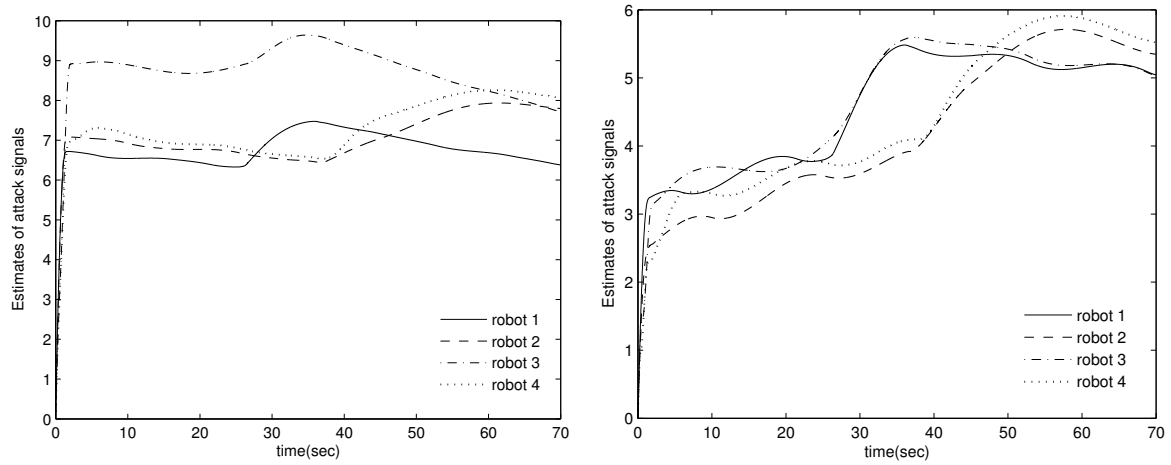

(**a**) $\hat{a}_{v,j}$ (**b**) $\hat{a}_{\omega,j}$

Figure 6. Estimates of attack signals.

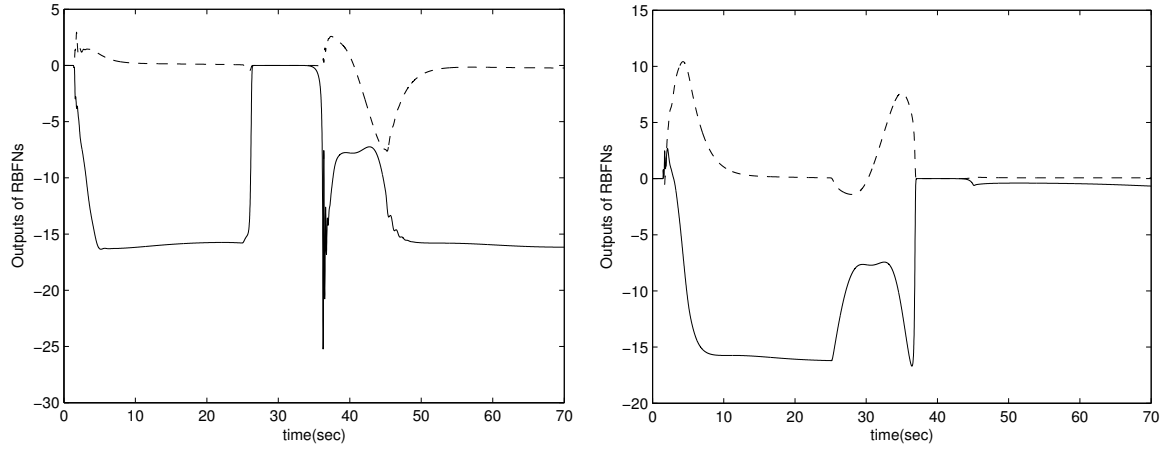

(**a**) Robot 1 (**b**) Robot 2

Figure 7. *Cont.*

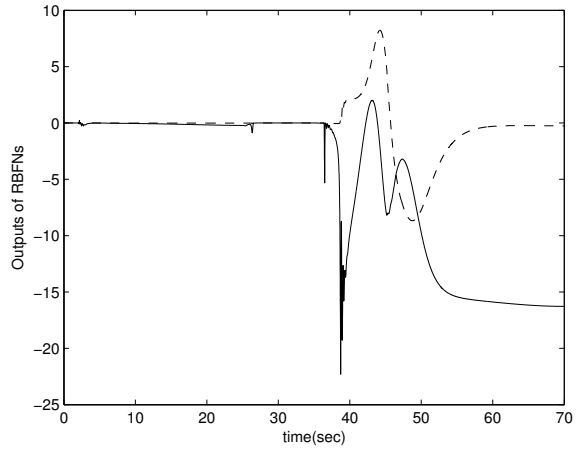

(**c**) Robot 3

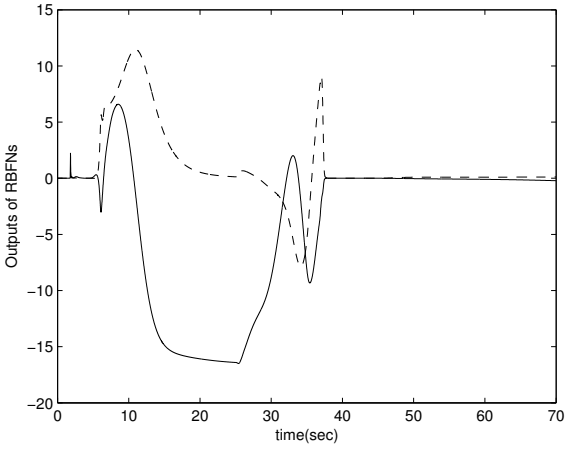

(**d**) Robot 4

Figure 7. Outputs of RBFNs (solid : $\widehat{W}_{1,j}^{\top}\Phi_j(X_j)$, dashed : $\widehat{W}_{2,j}^{\top}\Phi_j(X_j)$).

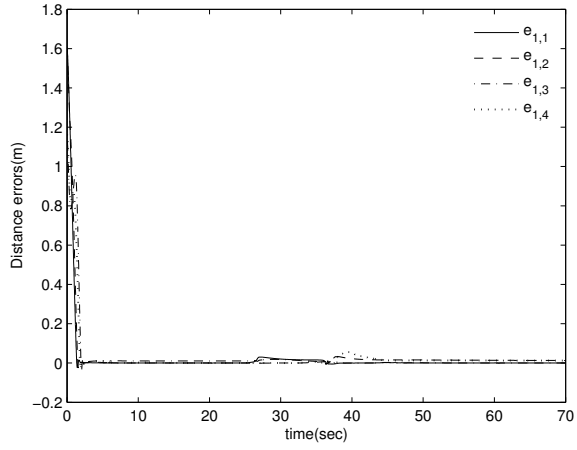

(**a**) Distance errors $e_{1,j}$

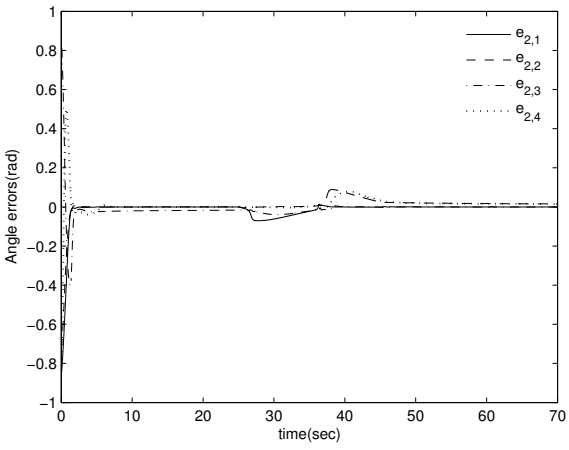

(**b**) Angle errors $e_{2,j}$

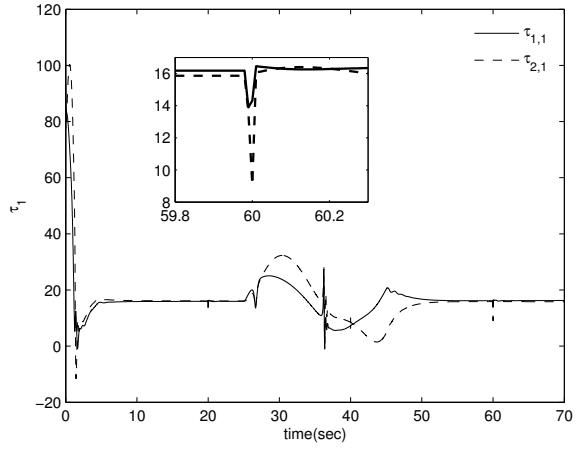

(**c**) τ_1

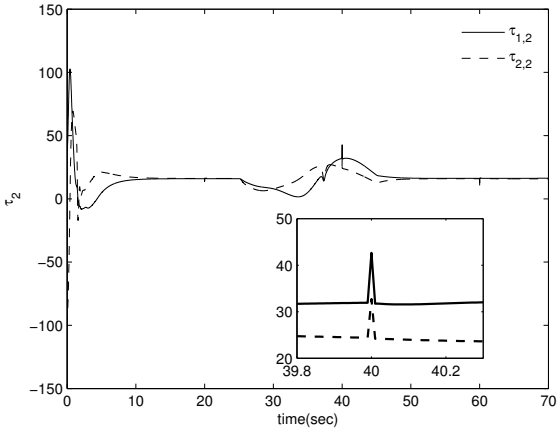

(**d**) τ_2

Figure 8. *Cont.*

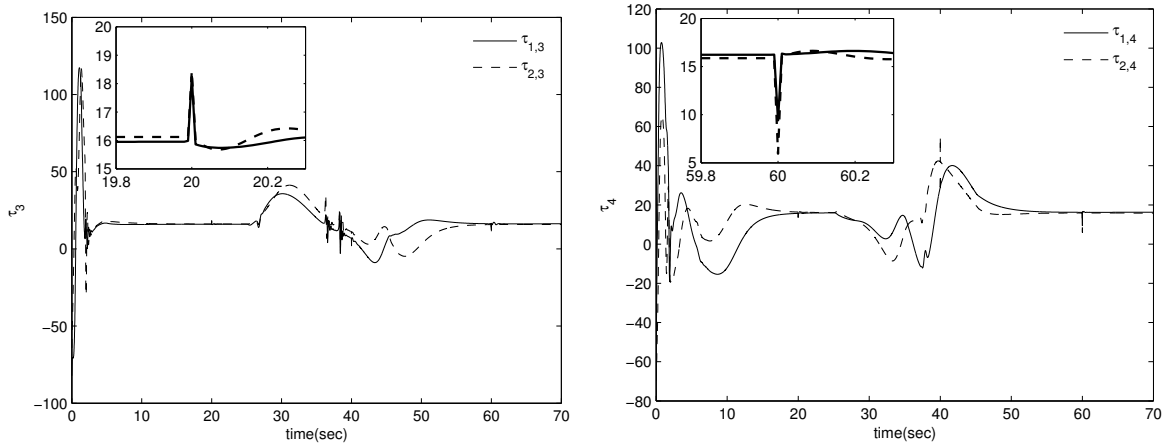

(**e**) τ_3 (**f**) τ_4

Figure 8. Simulation results for impulse attack signals.

5. Conclusions

In this paper, an adaptive secure control scheme has been proposed for achieving the leader-follower formation of nonholonomic mobile robots with uncertainty and deception attacks. It has been assumed that all follower robots receive their leader robot's information corrupted by malicious attacks through the network. The effects of the time-varying attack signals injected into the leader's information have been overcome by the adaptive technique, and the uncertainty arising from the dynamic model of nonholonomic mobile robots has been compensated by the RBFNs. From the Lyapunov stability theory, it has been proven that all estimation errors and formation tracking errors are bounded for all time. Because these errors can be reduced by adjusting the design parameters, the desired formation is achieved even though the leader's velocities corrupted by deception attacks are transmitted to the followers. Finally, simulation results have been presented to verify the effectiveness of the proposed theoretical result. Further studies on the state and input constraint problem and the collision avoidance problem under unknown deception attacks are recommended as future work.

Author Contributions: Conceptualization, B.-S.P. and S.-J.Y.; methodology, B.-S.P. and S.-J.Y.; software, B.-S.P.; validation, B.-S.P. and S.-J.Y.; formal analysis, B.-S.P. and S.-J.Y.; investigation, B.-S.P.; writing—original draft preparation, B.-S.P.; writing—review and editing, S.-J.Y.; supervision, S.-J.Y. All authors have read and agreed to the published version of the manuscript.

Funding: This research was supported by the National Research Foundation of Korea (NRF) grant funded by the Korea government (NRF-2019R1A2C1004898 and NRF-2019R1A2C1087552).

Institutional Review Board Statement: Not applicable.

Informed Consent Statement: Not applicable.

Data Availability Statement: Not applicable.

Conflicts of Interest: The authors declare no conflict of interest.

References

1. Amin, S.; Crdenas, A.A.; Sastry, S.S. Safe and secure networked control systems under denial-of-service attacks. In *Hybrid Systems: Computation and Control*; Springer: Berlin, Germany, 2009; pp. 31–45.
2. Corona, I.; Giacinto, G.; Roli, F. Adversarial attacks against intrusion detection systems: Taxonomy, solutions and open issues. *Inf. Sci.* **2013**, *239*, 201–225. [CrossRef]
3. Dolk, V.S.; Tesi, P.; Persis, C.; Heemels, W.P.M.H. Event-triggered control systems under denial-of-service attacks. *IEEE Trans. Control Netw. Syst.* **2017**, *4*, 93–105. [CrossRef]

4. Wang, J.X.; Liu, Z.X.; Zhang, S.G.; Zhang, X. Defending collaborative false data injection attacks in wireless sensor networks. *Inf. Sci.* **2014**, *254*, 39–53. [CrossRef]
5. He, W.; Gao, X.; Zhong, W.; Qian, F. Secure impulsive synchronization control of multi-agent systems under deception attacks. *Inf. Sci.* **2018**, *459*, 354–368. [CrossRef]
6. Ding, D.; Wang, Z.; Han, Q.L.; Wei, G. Security control for discrete-time stochastic nonlinear systems subject to deception attacks. *IEEE Trans. Syst. Man Cybern. Syst.* **2018**, *48*, 779–789. [CrossRef]
7. Zhu, M.H.; Martnez, S. On the performance analysis of resilient networked control systems under replay attacks. *IEEE Trans. Autom. Control* **2014**, *59*, 804–808. [CrossRef]
8. Ye, D.; Zhang, T.Y.; Guo, G. Stochastic coding detection scheme in cyber-physical systems against replay attack. *Inf. Sci.* **2019**, *481*, 432–444. [CrossRef]
9. Huang, J.S., Zhao, L.; Wang, Q.G. Adaptive control of a class of strict nonlinear systems under replay attacks. *ISA Trans.* **2020**, *107*, 134–142. [CrossRef]
10. Yucelen, T.; Haddad, W.M.; Feron, E.M. Adaptive control architecture for mitigating sensor attacks in cyber-physical systems. *Cyber-Phys. Syst.* **2016**, *2*, 24–52. [CrossRef]
11. Jin, X.; Haddad, W.M.; Yucelen, T. An adaptive control architecture for mitigating sensor and actuator attacks in cyber-physical systems. *IEEE Trans. Autom. Control* **2017**, *62*, 6058–6064. [CrossRef]
12. An, L.; Yang, G.H. Improved adaptive resilient control against sensor and actuator attacks. *Inf. Sci.* **2018**, *423*, 145–156. [CrossRef]
13. Yin, T,; Gu, A.Z. Security control for adaptive event-triggered networked control systems under deception attacks. *IEEE Access* **2020**, *9*, 10789–10796.
14. Mousavinejad, E.; Ge, X.; Han, Q.; Yang, F.; Vlacic, L. Resilient tracking control of networked control systems under cyber attacks. *IEEE Trans. Cybern.* **2021**, *51*, 2107–2119. [CrossRef]
15. Dong, L.; Xu, H.; Wei, X.; Hu, X. Security correction control of stochastic cyber-physical systems subject to false data injection attacks with heterogeneous effects. *ISA Trans.* **2021**, in press.
16. Yoo, S.J. Neural-network-based adaptive resilient dynamic surface control against unknown deception attack of uncertain nonlinear time-delay cyberphysical systems. *IEEE Tran. Neural Netw. Learn. Syst.* **2019**, *31*, 4341–4353. [CrossRef]
17. Yoo, S.J. Approximation-based event-triggered control against unknown injection data in full states and actuator of uncertain lower-triangular nonlinear systems. *IEEE Access* **2020**, *8*, 101747–101757. [CrossRef]
18. Yang, Y.; Huang, J.; Su, X.; Wang, K.; Li, G. Adaptive control of second-order nonlinear systems with injection and deception attacks. *IEEE Trans. Syst. Man Cybern. Syst.* **2021**, in press.
19. Zhang, K.; Su, R.; Zhang, H.; Tian, Y. Adaptive resilient event-triggered control design of autonomous vehicles with an iterative single critic learning framework. *IEEE Trans. Neural Netw. Learn. Syst.* **2021**, in press.
20. Balch, T.; Arkin, R.C. Behavior-based formation control for multi-robot teams. *IEEE Trans. Robot. Autom.* **1998**, *14*, 926–939. [CrossRef]
21. Lewis, M.A.; Tan, K.H. High precision formation control of mobile robots using virtual structures. *Auton. Robot.* **1997**, *14*, 387–403. [CrossRef]
22. Desai, J.P.; Ostrowski, J.; Kumar, V. Modeling and control of formations of nonholonomic mobile robots. *IEEE Trans. Robot. Autom.* **2001**, *17*, 905–908. [CrossRef]
23. Consolini, L.; Morbidi, F.; Prattichizzo, D.; Tosques, M. Leader-follower formation control of nonholonomic mobile robots with input constraints. *Automatica* **2008**, *44*, 1343–1349. [CrossRef]
24. Defoort, M.; Floquet, T.; Kokosy, A.; Perruquetti, W. Sliding-mode formation control for cooperative autonomous mobile robots. *IEEE Trans. Ind.* **2008**, *55*, 3944–3953. [CrossRef]
25. Dierks, T.; Jagannathan, S. Neural network control of mobile robot formations using RISE feedback. *IEEE Trans. Syst. Man Cybern.-Part B Cybern.* **2009**, *39*, 332–347. [CrossRef]
26. Poonawala, H.A.; Satici, A.C.; Exkert, H.; Spong, M.W. Collision-free formation control with decentralized connectivity preservation for nonholonomic wheeled mobile robots. *IEEE Trans. Control. Syst. Technol.* **2015**, *2*, 122–130. [CrossRef]
27. Wang, Y.; Wang, D.; Yang, S.; Shan, M. A practical leader-follower tracking control scheme for multiple nonholonomic mobile robots in unknown obstacle environments. *IEEE Trans. Control Syst. Technol.* **2019**, *27*, 1685–1693. [CrossRef]
28. Kan, Z.; Klotz, J.R.; Shea, J.M.; Doucette, E.A.; Dixon, W.E. Decentralized rendezvous of nonholonomic robots with sensing and connectivity constraints. *J. Dyn. Syst. Meas. Control* **2017**, *39*, 024501. [CrossRef]
29. Park, B.S.; Yoo, S.J. Connectivity-maintaining obstacle avoidance approach for leader-follower formation tracking of uncertain multiple nonholonomic mobile robots. *Expert Syst. Appl.* **2021**, *171*, 114589. [CrossRef]
30. Fukao, T.; Nakagawa, H.; Adachi, N. Adaptive tracking control of a nonholonomic mobile robot. *IEEE Trans. Robot. Autom.* **2000**, *16*, 609–615. [CrossRef]
31. Fawzi, H.; Tabuada, P.; Diggavi, S. Secure estimation and control for cyber-physical systems under adversarial attacks. *IEEE Trans. Autom. Control* **2014**, *59*, 1454–1467. [CrossRef]
32. Li, L.; Yang, H.; Xia, Y.; Zhu, C. Attack detection and distributed filtering for state-saturated systems under deception attack. *IEEE Trans. Control Netw. Syst.* **2021**, in press.
33. Ge, S.S.; Wang, C. Adaptive neural control of uncertain MIMO nonlinear systems. *IEEE Trans. Neural Netw.* **2004**, *15*, 674–692. [CrossRef]

34. Polycarpou, M.M. Stable adaptive neural control scheme for nonlinear systems. *IEEE Trans. Autom. Control* **1996**, *41*, 447–451. [CrossRef]
35. Swaroop, D.; Hedrick, J.K.; Yip, P.P.; Gerdes, J.C. Dynamic surface control for a class of nonlinear systems. *IEEE Trans. Autom. Control* **2000**, *45*, 1893–1899. [CrossRef]
36. Tanner, H.G.; Pappas, G.J.; Kumar, V. Leader-to-formation stability. *IEEE Trans. Robot. Autom.* **2004**, *20*, 443–455. [CrossRef]